

## DYNAMIC ANALYSIS OF HIGH-SPEED RAILWAY BRIDGES THROUGH A THIN-WALLED BEAM ELEMENT

Diego Lisi<sup>1</sup>, Ricardo F. Vieira\*<sup>2</sup>, Francisco B. Virtuoso<sup>2</sup>

<sup>1</sup>Instituto Superior Técnico - Politecnico di Milano  
{diegolisi1987}@gmail.com

<sup>2</sup>Instituto Superior Técnico - Universidade Técnica de Lisboa  
{ricardo.figueiredo.vieira,francisco.virtuoso}@ist.utl.pt

**Keywords:** bridge dynamics, moving loads, thin-walled beams, warping, lateral-torsional coupled vibration.

**Abstract.** *The cross-section warping of bridge cross-section due to the passage of high-speed trains can be a relevant aspect to consider in the dynamic analysis of bridges, particularly because of the usual railway lines layout. A thin-walled beam model that includes cross-section warping is derived for the dynamic analysis of bridges submitted to moving loads as an alternative to three-dimensional shell elements. The model is applied to the evaluation of the free vibration frequencies taking in account the coupling between flexural and torsional vibration modes. An application to a continuous bridge with three spans submitted to a moving load is presented.*

## 1 INTRODUCTION

A thin-walled beam model for the dynamic analysis of bridges due to the passage of high-speed trains is presented in this paper. The beam model considers the cross-section warping which is considered relevant given the usual layout for double lane railway lines. Relatively to a three-dimensional shell finite element models, the thin-walled beam model has not only the advantage of reproducing warping effects with simpler models, but also to allow a more simple interpretation of results.

The dynamic behaviour of thin-walled beam whenever the mass centre does not coincide with the corresponding cross-section shear centre results in a coupled vibration between the flexural and torsional mode. The coupled between flexure and torsion in free vibration has been analytically studied for single span beams with different support conditions by [10, 6], which has evaluated the influence of the warping stiffness in the natural frequencies, being more recently several analytical solution for the problem presented by [9, 1, 8]. The dynamic analysis of continuous beams through analytical methods is somewhat limited and therefore the approach through a dynamic stiffness matrix has been usually adopted, [4, 2]. The analysis due to the action of moving loads was described by [10] and more recently thoroughly studied by [5]. However, the coupled flexural-torsional vibration including warping was, to the best knowledge of the authors, only studied analytically by [7] for a simple supported beam.

A thin-walled beam model that considers the cross-section warping as an additional degree of freedom is derived and applied to the analysis of bridges submitted to moving loads. The finite element is derived by adopting a single axis which is coincident with the cross-section centroid, having 7 degrees of freedom per node. The presented model is adopted for the analysis of a railway bridge submitted to the passage of high-speed trains, which are modeled by a single load.

## 2 DYNAMIC FORMULATION OF THIN-WALLED BEAMS

The thin-walled beam dynamic formulation considering the cross-section warping and admitting a linear-elastic material behaviour is presented. The Euler-Bernoulli hypotheses are assumed to remain valid and the cross-section is considered to be transversely rigid. The displacement field components represented in Fig. 1 are defined by: (i) 4 degrees of freedom in the longitudinal direction that represent the axial displacement of  $C$  (coincident with the mass centre of the cross-section),  $\eta(x)$ , the cross-section rotation around principal axes,  $\xi'_y(x)$  e  $\xi'_z(x)$ , and the cross-section warping,  $\omega$ ; and (ii) 3 degrees of freedom that represent the translation of the cross-section  $\xi_y(x)$  e  $\xi_z(x)$ , and the rotation  $\varphi(x)$  around a generic point  $P = (y_P, z_P)$ , as represented in Fig. 2.

The cross-section warping is defined through the classic theory of thin-walled structures by [11] through the sectorial coordinate of the cross-section, being the displacement field for the cross-section profile defined as follows:

$$u_x(x, y, z) = \eta(x) - (y - y_P)\xi'_y(x) - (z - z_P)\xi'_z(x) - \omega_P(s)\varphi'(x) \quad (1)$$

$$u_y(x, y, z) = \xi_y(x) - (z - z_P)\varphi(x) \quad (2)$$

$$u_z(x, y, z) = \xi_z(x) + (y - y_P)\varphi(x) \quad (3)$$

Considering the displacements defined by Eq. (1) and assuming valid the small displacement

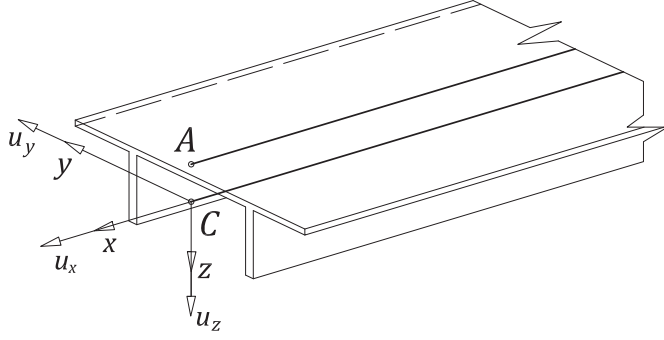


Figure 1: Thin-walled beam.

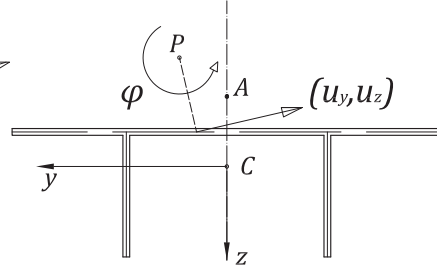


Figure 2: Sectorial coordinate.

hypothesis, the deformation components are defined by:

$$\varepsilon_x = \eta'(x) - (y - y_P)\xi_y''(x) - (z - z_P)\xi_z''(x) - \omega_P(s)\varphi''(x) \quad (4)$$

$$\gamma_{xs} = 2n\varphi(x)' \quad (5)$$

being the corresponding stress components obtained through an uniaxial constitutive law assuming a linear elastic behaviour of the material.

The dynamic equilibrium equations are obtained by applying the Hamilton principle as follows:

$$\int_{t_1}^{t_2} \delta(T - V)dt = \int_{t_1}^{t_2} \left( \frac{\partial T}{\partial q_i} \delta q_i + \frac{\partial T}{\partial \dot{q}_i} \delta \dot{q}_i + \frac{\partial T}{\partial \dot{q}_i'} \delta \dot{q}_i' - \frac{\partial V}{\partial q_i} \delta q_i - \frac{\partial V}{\partial \dot{q}_i} \delta \dot{q}_i - \frac{\partial V}{\partial \dot{q}_i''} \delta \dot{q}_i'' \right) dt = 0 \quad (6)$$

where  $V$  and  $T$  represent, respectively, the potential and the kinetic energy associated with the thin-walled beam, which can be written in terms of the displacements defined by Eq. (1); the variables  $q_i$  represent the generalized coordinate that define the beam displacement field, being defined as: (i)  $\delta\eta, \delta\eta'$  in the longitudinal direction, (ii)  $\delta\xi_y, \delta\xi_y', \delta\xi_y''$  e  $\delta\xi_z, \delta\xi_z', \delta\xi_z''$  for the flexure around the two axes and (iii)  $\delta\varphi, \delta\varphi', \delta\varphi''$  for the beam torsion. The potential energy of the beam is defined by:

$$V = U - W \text{ com } U = \frac{1}{2}(E\varepsilon_x^2 + G\gamma_{xs}^2) \quad \text{e} \quad W = p_x u_x + p_y u_y + p_z u_z \quad (7)$$

being  $U$  the deformation energy associated with the deformation components defined in (4) and (5);  $W$  represents the work of the applied forces, being  $p_x, p_y$  and  $p_z$  the corresponding volume densities along  $x, y$  e  $z$ , respectively. The beam kinetic energy is defined as follows:

$$T = \frac{1}{2} \int_{\Omega} \rho(\dot{u}_x^2 + \dot{u}_y^2 + \dot{u}_z^2) d\Omega \quad (8)$$

where  $\rho$  represents material mass density.

Substituting the deformation components (4) e (5) into the potential energy definition (7), and considering the velocity components associated with the displacement field (1) and (3) in the definition of the kinetic energy, the following expressions are obtained for the potential and kinetic energy:

$$V = \int_0^L \mathcal{F}_V [\eta, \eta', \xi_y, \xi_z, \varphi, \xi_y', \xi_z', \varphi', \xi_y'', \xi_z'', \varphi''] dL \quad T = \int_0^L \mathcal{F}_T [\dot{\eta}, \dot{\xi}_y, \dot{\xi}_z, \dot{\varphi}, \dot{\xi}_y', \dot{\xi}_z', \dot{\varphi}'] dL \quad (9)$$

beng  $\mathcal{F}_V$  and  $\mathcal{F}_V$  functionals defined by:

$$\begin{aligned} \mathcal{F}_T = & \frac{1}{2}\rho(A\dot{\eta}^2 - \dot{\eta}S_y^P\dot{\xi}_y - \dot{\eta}S_z^P\dot{\xi}_z - \dot{\eta}S_\omega^P\dot{\varphi}' - S_y^P\dot{\xi}_y\dot{\eta} + I_y^P\dot{\xi}_y'^2 + I_{yz}^P\dot{\xi}_y'\dot{\xi}_z' + I_{y\omega}^P\dot{\xi}_y'\dot{\varphi}' \\ & - S_z^P\dot{\xi}_z\dot{\eta} + I_{zy}^P\dot{\xi}_z\dot{\xi}_y + I_z^P\dot{\xi}_z'^2 + I_{z\omega}^P\dot{\xi}_z'\dot{\varphi}' - S_\omega^P\dot{\varphi}(x)'\dot{\eta} + I_{\omega y}^P\dot{\varphi}'\dot{\xi}_y + I_{\omega z}^P\dot{\varphi}(x)'\dot{\xi}_z + I_{\omega\omega}^P\dot{\varphi}'^2 \\ & + A\dot{\xi}_y^2 - 2\dot{\xi}_yS_z^P\dot{\varphi} + I_z^P\dot{\varphi}^2 + A\dot{\xi}_z^2 + 2\dot{\xi}_zS_y^P\dot{\varphi} + I_y^P\dot{\varphi}^2) \end{aligned} \quad (10)$$

$$\begin{aligned} \mathcal{F}_T = & \frac{1}{2}\rho(A\dot{\eta}^2 - \dot{\eta}S_y^P\dot{\xi}_y - \dot{\eta}S_z^P\dot{\xi}_z - \dot{\eta}S_\omega^P\dot{\varphi}' - S_y^P\dot{\xi}_y\dot{\eta} + I_y^P\dot{\xi}_y'^2 + I_{yz}^P\dot{\xi}_y'\dot{\xi}_z' + I_{y\omega}^P\dot{\xi}_y'\dot{\varphi}' \\ & - S_z^P\dot{\xi}_z\dot{\eta} + I_{zy}^P\dot{\xi}_z\dot{\xi}_y + I_z^P\dot{\xi}_z'^2 + I_{z\omega}^P\dot{\xi}_z'\dot{\varphi}' - S_\omega^P\dot{\varphi}(x)'\dot{\eta} + I_{\omega y}^P\dot{\varphi}'\dot{\xi}_y + I_{\omega z}^P\dot{\varphi}(x)'\dot{\xi}_z + I_{\omega\omega}^P\dot{\varphi}'^2 \\ & + A\dot{\xi}_y^2 - 2\dot{\xi}_yS_z^P\dot{\varphi} + I_z^P\dot{\varphi}^2 + A\dot{\xi}_z^2 + 2\dot{\xi}_zS_y^P\dot{\varphi} + I_y^P\dot{\varphi}^2) \end{aligned} \quad (11)$$

in which  $A$  represent the cross-section area;  $S_{\alpha\beta}^P$  and  $I_{\alpha\beta}^P$ , com  $\alpha, \beta = y, z, \omega$ , represent the first a second order moment of area.

The dynamic equilibrium equations of the thin-walled beam are obtained by introducing Eq. (9) into (6), performing an integration of the velocity dependent terms and an integration by parts along the beam axis. Considering the centroid and the shear centre of the cross-section, the following equilibrium equations are obtained:

Extension

$$-\rho A \frac{\partial^2 \eta}{\partial t^2} + EA \frac{\partial^2 \eta}{\partial x^2} + q_x = 0 \quad (12)$$

Flexure ( $x, y$ )

$$\frac{\partial^2 M_y}{\partial x^2} + \frac{\partial m_y}{\partial x} + q_y - \rho A \frac{\partial^2 \xi_y}{\partial t^2} + \rho S_z^A \frac{\partial^2 \varphi}{\partial t^2} + \rho I_y \frac{\partial^2 \xi_y''}{\partial t^2} = 0 \quad (13)$$

Flexure ( $x, z$ )

$$\frac{\partial^2 M_z}{\partial x^2} + \frac{\partial m_z}{\partial x} + \rho I_z \frac{\partial^2 \xi_z''}{\partial t^2} \frac{\partial V_z}{\partial x} + q_z - \rho A \frac{\partial^2 \xi_z}{\partial t^2} - \rho S_y^A \frac{\partial^2 \varphi}{\partial t^2} = 0 \quad (14)$$

Torsion

$$M_x = \rho I_{\omega\omega} \frac{\partial^2}{\partial t^2} \left( \frac{\partial \varphi}{\partial x} \right) + \frac{\partial M_\varphi}{\partial x} + M_x^{sv} + b \quad (15)$$

$$\frac{dM_x}{dx} - \rho(I_z^A + I_y^A) \frac{\partial \varphi^2}{\partial t^2} + \rho S_z^A \frac{\partial^2 \xi_y}{\partial t^2} - \rho S_y^A \frac{\partial^2 \xi_z}{\partial t^2} + m_\varphi = 0 \quad (16)$$

Although considering the torsion referred to the cross-section shear centre, the dynamic equilibrium equations of the beam are still coupling the beam flexural and torsional behaviour. Therefore, a single axis for the dynamic analysis of thin-walled beams can be adopted, which renders the model more efficient to implement.

### 3 THIN-WALLED FINITE ELEMENT

#### 3.1 Formulation

A finite element is derived for the solution of the thin-walled beam differential equations by considering the displacement field interpolation functions to be also adopted as weight functions so as to derive the corresponding discrete equations. The derived finite element considers an additional degree of freedom for the cross section warping, which is henceforth applied to the dynamic analysis of thin-walled beams.

The approximation of the displacement field for the beam finite element is defined as follows:

$$\eta^e(x) = \mathbf{N}^e \mathbf{u}_x^e \quad \xi_y^e(x) = \mathbf{H}_y^e \mathbf{u}_y^e \quad \xi_z^e(x) = \mathbf{H}_z^e \mathbf{u}_z^e \quad \varphi^e(x) = \mathbf{H}_\varphi^e \mathbf{u}_\varphi^e \quad (17)$$

where  $\mathbf{N}^e$  and  $\mathbf{H}_\gamma^e$ , with  $\gamma = y, z, \varphi$ , represent sets of linear Lagrange and Hermite functions that are adopted as approximation functions; the corresponding amplitudes are set to represent the nodal displacements of the element as represented in Fig. 3, being defined as follows,

$$\mathbf{u}_x^e = [ \eta_1^e \quad \eta_2^e ]^t \quad \mathbf{u}_y^e = [ \xi_{y1}^e \quad \xi_{y1}^{\prime e} \quad \xi_{y2}^e \quad \xi_{y2}^{\prime e} ]^t \quad (18)$$

$$\mathbf{u}_z^e = [ \xi_{z1}^e \quad \xi_{z1}^{\prime e} \quad \xi_{z2}^e \quad \xi_{z2}^{\prime e} ]^t \quad \mathbf{u}_\varphi^e = [ \varphi_1^e \quad \varphi_1^{\prime e} \quad \varphi_2^e \quad \varphi_2^{\prime e} ]^t \quad (19)$$

The undamped dynamic equilibrium of the thin-walled beam element is defined through the following system of algebraic equations,

$$\mathbb{M}_e \ddot{\mathbf{d}}_e + \mathbb{K}_e \mathbf{d}_e - \mathbf{f}_e = \mathbf{0} \quad (20)$$

where the matrices  $\mathbb{M}^e$  and  $\mathbb{K}^e$  represent, respectively, the mass and the stiffness element matrices and  $\mathbf{f}^e$  the element vector of external forces. The element nodal displacements are represented by  $\mathbf{d}^e$ , having 14 components, which corresponds to 7 degrees of freedom per each end.

The global equations of a model are obtained by the assemblage of the corresponding mass and stiffness element matrices by guaranteeing the compatibility between elements in terms of nodal displacements.

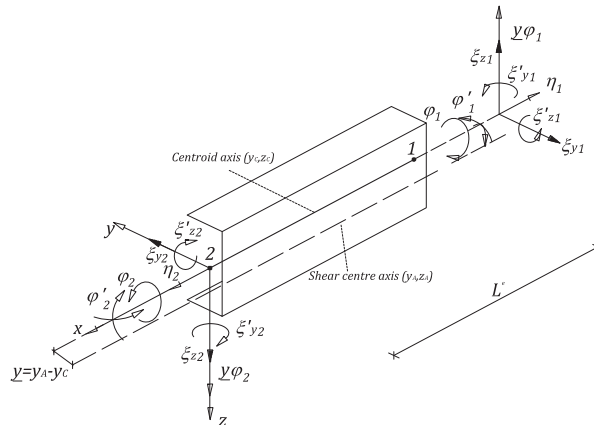


Figure 3: Thin-walled finite element.

### 3.2 Dynamic analysis

The dynamic analysis of the combined flexural-torsional vibration for multi-span continuous bridges is considered through the developed thin-walled beam model by finite element derived.

The natural frequencies and the corresponding vibration modes are obtained through the equilibrium equations of the model by assuming the motion undamped. By considering a solution based on a sinusoidal function for the global equilibrium equations (obtained from the assemblage of Eqs. 20), the following linear eigenvalue problem is obtained:

$$(\mathbb{K} - p^2 \mathbb{M}) \phi = \mathbf{0} \quad (21)$$

where  $\mathbb{M}$  and  $\mathbb{K}$  represent the global matrices of mass and stiffness respectively. The natural frequency corresponds to the eigenvalue  $p$ , being the respective vibration mode defined through the corresponding eigenvector,  $\phi$ .

Considering the damping effect, the dynamic equilibrium equations due to a moving load,  $\mathbf{f}$ , can be written in the following form:

$$\mathbb{M} \ddot{\mathbf{d}} + \mathbb{C} \dot{\mathbf{d}} + \mathbb{K} \mathbf{d} - \mathbf{f} = \mathbf{0} \quad (22)$$

which can be rewritten by taking advantage of the orthogonality conditions between the vibration modes obtained from Eq. (21). In fact, the Eq. (22) can be written in an uncoupled form by adopting for coordinates the vibration modes obtained by defining the damping matrix in Eq. (22) as a linear combination of the mass and the stiffness matrices. The solution of Eq. (22) is then performed through the solution of a set of systems with one degree of freedom:

$$M_n \ddot{d}_n + C_n \dot{d}_n + K_n d_n = f_n(t) \quad (23)$$

by adopting the time-step method for the time integration defined by *Newmark*. The response is then obtained from modal superposition as follows:

$$\mathbf{d}(t) = \phi_1 d_1 + \phi_2 d_2 + \dots + \phi_n d_n + \dots \quad (24)$$

## 4 APPLICATIONS

The thin-walled beam model is applied to the analysis of a railway bridge for high-speed trains. A continuous bridge with three spans ( $30\text{ m} + 40\text{ m} + 30\text{ m}$ ) is analyzed by the beam model represented in Fig. 4, being the torsion prevented at the end supports. The bridge is made of a concrete with an elastic modulus of  $E = 32\text{ GPa}$ , being admitted two cross-section geometries with an equivalent flexural stiffness: a double-tee and a box girder cross-section. The sections are depicted in Figs. 6 and 5, respectively, being the corresponding dimensions and characteristics given in tables 1 and 2.

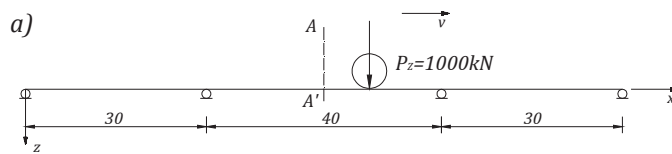


Figure 4: Bridge model.

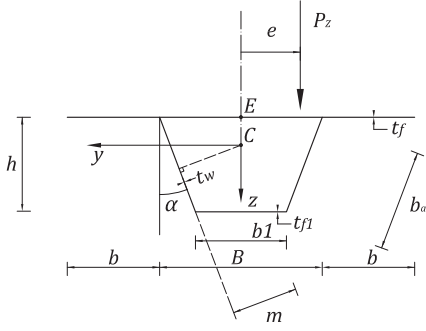


Figure 5: Box girder cross-section.

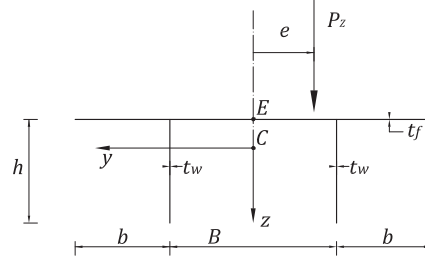


Figure 6: Double-Tee cross-section.

Table 1: Cross-section dimensions.

	$B$ [m]	$b$ [m]	$t_w$ [m]	$t_f$ [m]	$t_{f1}$ [m]	$\alpha$	$h$ [m]
<b>Box girder cross-section</b>	7.30	3.00	0.50	0.35	0.30	$23^\circ$	2.28
<b>Double-Tee cross-section</b>	6.65	3.33	0.80	0.35			3.03

Table 2: Cross-section characteristics.

	$A$ [m <sup>2</sup> ]	$I_y$ [m <sup>4</sup> ]	$I_z$ [m <sup>4</sup> ]	$I_{\omega\omega}$ [m <sup>6</sup> ]	$K$ [m <sup>4</sup> ]
<b>Box girder cross-section</b>	8.74	7.84	97.50	12.06	17.14
<b>Double-Tee cross-section</b>	9.51	9.16	122.37	110.14	1.17

A numerical model with 100 elements for the central span and 75 elements for the lateral spans is considered for the analysis. The natural frequencies are obtained by the solution of the eigenvalue problem stated in (21), where both the stiffness and the mass matrices take into account the warping degree of freedom. The mass associated with the structural and non-structural weight was considered through appropriate densities.

The frequencies obtained are presented in table (3) for both cross-sections, being identified the corresponding vibrational mode. The behaviour of the two cross-sections is significantly different inasmuch as for the open cross-section the coupled vibrational modes occur for lower frequencies (namely, the 2<sup>nd</sup> mode, with 4.81Hz), whereas for the box girder the first coupled mode corresponds to a natural frequency of 10.68 Hz.

The bridge is submitted to a moving load of 1000 kN in order to simulate the passage of a train. The load is applied with an eccentricity  $e = 2.5$  m as represented in Figs. 5 and 6 which corresponds approximately to the position of the railway track for both cross-sections. A damping coefficient of  $\xi = 0.01$  is considered, being derived a proportional damping matrix. The dynamic response of the bridge is obtained by a superposition of the results given from the Newmark integration of the modal equations.

The bridge dynamic response is evaluated through a set of dynamic influence lines regarding the bridge displacements. The influence lines for the torsion and the transverse displacements of the mid-span cross section are obtained for different speeds of the load passage, being the results represented in Figs. 7 and Fig. 8 for the double-tee and box girder cross-section, respectively. A comparison between the influence lines of mid-span torsion for the two types of cross-section is represented in Fig. 9, in which is verified that the flexural-torsional coupled vibration is more relevant for the open cross-section than for the box girder.

The dynamic response of the double-tee cross-section bridge is obtained with and without the cross-section warping stiffness towards an evaluation of the corresponding influence. The

Table 3: Bridge model natural frequencies.

Mode	Double Tee		Box girder	
	Freq. [Hz]	Vibrational mode	Freq. [Hz]	Vibrational mode
1	<b>3.97</b>	$u_z$	<b>3.79</b>	$u_z$
2	<b>4.81</b>	$u_y - \varphi$ coupled	<b>6.19</b>	$u_z$
3	<b>6.49</b>	$u_z$	<b>7.43</b>	$u_z$
4	<b>7.37</b>	$u_y - \varphi$ coupled	<b>9.08</b>	$u_x$
5	<b>7.79</b>	$u_z$	<b>10.68</b>	$u_y - \varphi$ coupled
6	<b>8.52</b>	$u_y - \varphi$ coupled	<b>14.16</b>	$u_z$
7	<b>9.08</b>	$u_x$	<b>14.22</b>	$u_y - \varphi$ coupled
8	<b>14.84</b>	$u_z$	<b>14.37</b>	$u_y - \varphi$ coupled
9	<b>15.81</b>	$u_y - \varphi$ coupled	<b>17.01</b>	$u_y - \varphi$ coupled
10	<b>17.34</b>	$u_y - \varphi$ coupled	<b>21.50</b>	$u_z$
11	<b>22.51</b>	$u_z$	<b>22.32</b>	$u_y - \varphi$ coupled
12	<b>23.64</b>	$u_y - \varphi$ coupled	<b>23.44</b>	$u_z$
13	<b>24.55</b>	$u_z$	<b>26.17</b>	$u_y - \varphi$ coupled
14	<b>25.61</b>	$u_y - \varphi$ coupled	<b>27.25</b>	$u_x$
15	<b>27.25</b>	$u_x$	<b>29.80</b>	$u_y - \varphi$ coupled

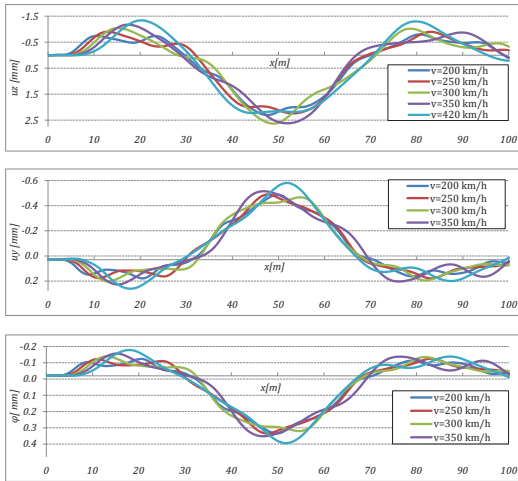


Figure 7: Dynamic influence lines for the mid-span central section (Double-Tee cross-section).

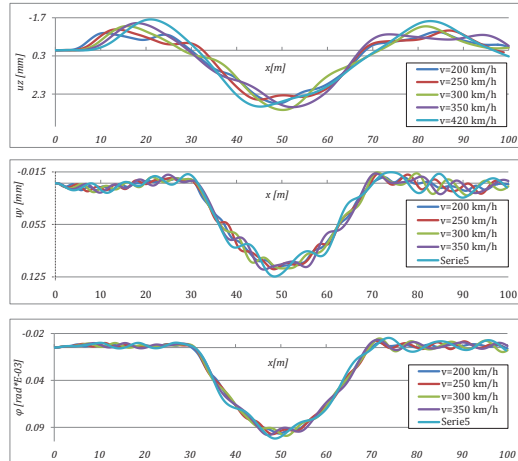


Figure 8: Dynamic influence lines for the mid-span central section (Box girder cross-section).

vertical displacements of the cross-section loaded point are presented in Fig. 10, verifying that neglect warping result in a significant increase of displacements.

Static influence lines of the lateral displacement and the torsion of the bridge are compared with the correspondent dynamic lines in Fig. 11, being verified that the dynamical behaviour corresponds to a relevant amplification effect on the response of the bridge to the moving load.



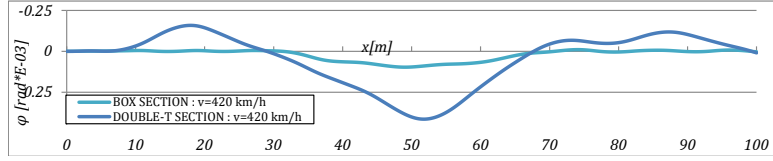


Figure 9: Comparison between the cross-section torsion (speeds of 420 km/h and 200 km/h).

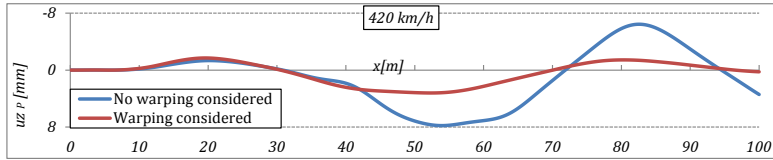


Figure 10: Dynamic influence lines for the midspan central section  $u_z^P$  (vertical displacement of the loading point)

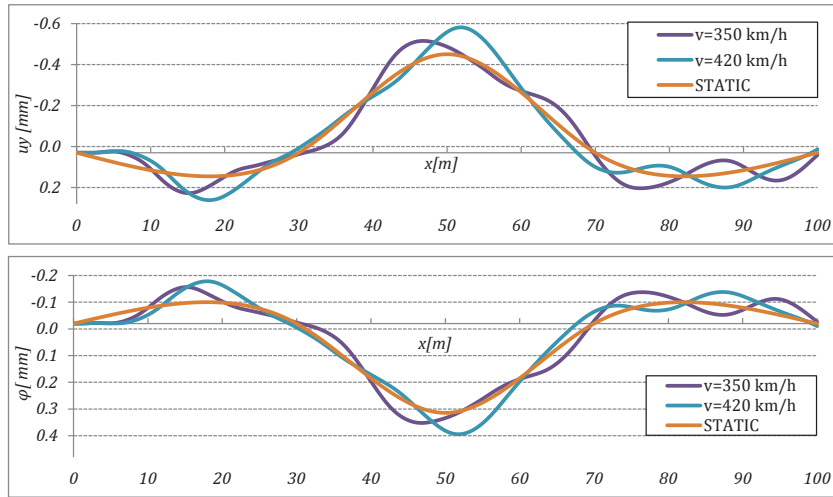


Figure 11: Static and dynamic influence lines for the midspan central section - transverse displacement and rotation.

## 5 CONCLUSIONS

A thin-walled beam model for the dynamic analysis of railway bridges that considers the coupled flexural-torsional vibration modes was presented. The formulation considers the cross-section warping and neglects its in-plane deformation. The model was derived by adopting a single axis since in dynamics the coupling between flexure and torsion remains even when adopting the cross-section shear centre as a reference.

The thin-walled beam model was applied to the dynamic analysis of a three span continuous bridge considering two types of cross-sections with similar flexural stiffnesses: a double-tee and a box girder cross-section. The train was considered through the application of a single moving load traveling at constant speed, being the train mass as well as the interaction between the vehicle and the structure neglected.

The bridge natural frequencies and the corresponding vibration modes were obtained through the developed model for both cross-sections, being verified that the coupled modes for the

closed cross-section correspond to higher natural frequencies by comparison with those obtained for the open cross-section.

The dynamic influence lines for the displacements of the bridge cross-sections were obtained for both cross-section types and admitting the passage of the moving load at different speeds. The flexural-torsional coupled vibration was verified to be more relevant for the bridge with the open cross-section, being the response significantly influenced by the cross-section warping stiffness.

## REFERENCES

- [1] Arpaci, A. S.E. and Bozdog, E. and Sunbuloglu Triply coupled vibrations of thin-walled open cross-section beams including rotary inertia effects *Journal of Sound and Vibration*, 260:889–900, 2003.
- [2] Banerjee, J.R. Dynamic stiffness formulation for structural elements: A general approach *Computers and structures*, 63:101-103, 1997.
- [3] Lisi, D. A beam finite element including warping. *Thesis for Master degree in Structural Engineering*. (<https://www.politesi.polimi.it/handle/10589/66762?mode=simple>), 2012.
- [4] Friberg, P. O. Coupled Vibration of beams - an exact dynamic element stiffness matrix *International Journal For Numerical Methods in Engineering*, 19:479–493, 1983.
- [5] Fryba, L. Vibrations of solids and structures under to moving loads. Thomas Telford, 1999.
- [6] Gere, J. M. and Lin, Y. K. Coupled vibration of thin-walled beams of open cross section *Journal of Applied mechanics*, 25:373–378, 1958.
- [7] Michaltsos, G.T., Sarantithou, E. and Sophianopoulos, D.S. Flexural, Ätorsional vibration of simply supported open cross-section steel beams under moving loads *Journal of Sound and Vibration*, 280:479-494, 2005.
- [8] Prokic, A. On triply coupled vibrations of thin-walled beams with arbitrary cross-section *Journal of Sound and Vibration*, Volume 279, Issues 3-5, 21, 723-737, 2005.
- [9] Tanaka, M. and Bercin, A. N. Free vibration solution for uniform beams of nonsymmetrical cross section using Mathematica *Computers and structures*, 71:1–8, 1999.
- [10] Timoshenko, S.P. Young, D.H. W. Weaver Vibration Problems in Engineering, Wiley, New York, 1974.
- [11] Vlassov, V. Thin-Walled Elastic Beams. Israel program for scientific translations, Jerusalem, 1961.